Synthesis of a hole-containing polypyrrole film modified by copper cementation

I. L. Lehr, S. B. Saidman

Departamento De Ingeniería Química, Universidad Nacional Del Sur, Instituto De Ingeniería Electroquímica Y Corrosión (INIEC), Av. Alem 1253, Bahía Blanca 8000, Argentina
Correspondence to: S. B. Saidman (E-mail: ssaidman@criba.edu.ar)

ABSTRACT: A simple procedure enables to obtain a hole-containing PPy film on SAE 4140 steel in sodium bis(2-ethylhexyl) sulfosuccinate (AOT) solutions. The film characterization was made by electrochemical and morphological studies. The effects of electropolymerization parameters on the obtained morphology are discussed. The formation of the coating is conditioned by the nature of the substrate and surfactant and the electrochemical technique employed. Electrochemical investigations demonstrate that the hole-containing PPy film presents an increase in surface area. The polymer was modified by cementation of copper particles. The modified polymer offers a higher electrocatalytic activity for the HER than usual PPy. © 2016 Wiley Periodicals, Inc. J. Appl. Polym. Sci. **2016**, *133*, 43650.

INTRODUCTION

Polypyrrole is one of the conducting polymers which has been extensively investigated due to its physicochemical stability, high conductivity, easy processability, and relatively low cost.[1–5] The incorporation of metal particles into the polymeric matrix has received considerable attention due to the potential applications of these composites in catalytic materials,[6,7] microelectronic devices,[8,9] chemical sensors,[10,11] and protection against corrosion.[12,13] Ag,[14,15] Cu,[16,17] and Au[18,19] are among the metals used to modify polymers.

Electrochemical techniques are commonly used to modify polymers with metals because they allow controlling both the amount of metallic particles deposited on the polymer film and the morphology of the coating. It has been demonstrated that the size and the amount of deposited particles and their location (in whole or in the top) in the polymer film can determine the electrochemical behavior of these coatings. Moreover, the structure and morphology of the polymer have significant influence on the metal deposition process and the properties of the metallic phase within the polymer matrix. Tsakova *et al.* demonstrated that the thickness and the redox state of polyaniline influence the number, size and location of deposited copper particles.[20] These authors also reported that the metal phase nucleation occurs preferentially at active sites in the polymer film. These sites are located in the micropores of the polymer matrix. The metal clusters continue to grow through the polymer, sealing the micropores and finally covering the film.

On the other hand, electrochemically prepared PPy films are particularly attractive for electrocatalytic reductions.[6,21–27] Multilayered polymeric coatings provide three-dimensional reaction sites on the electrode. Several works have been reported that the metallic particles incorporation into porous matrices increases the specific area of these materials and thus improves catalytic efficiency. Saidani *et al.* have been published that copper dispersed onto PPy films acts as an electrocatalyst for the proton reduction.[16,28]

One of the most important goals of current research is the removal of heavy metals of the wastewater. Copper is considered as one of the most toxic metals and possesses a potential threat to the human health and environment, even at low concentrations. Wastewater from various industries, such as electroplating, plastic, metal finishing, pigments, and mining contains copper. In this regard, cementation is one of the most effective and economic technique for recovering toxic and/or valuable metals from industrial waste solution because of its simplicity and ease of implementation.

Previous works have shown that an AOT-containing solution can be used for the electrosynthesis of stable, adherent, and homogeneous films onto Al,[29] Fe,[30] Ti,[31] and SAE 4140 steel.[32] Sodium bis(2-ethylhexyl) sulfosuccinate, also known as AOT, is an anionic surfactant widely used in the formation of reverse
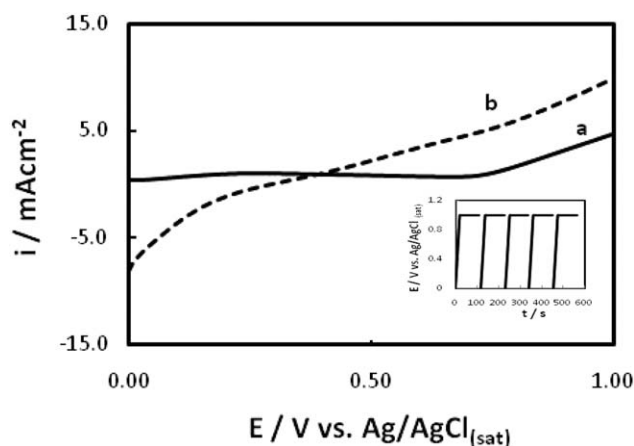
Figure 1. Linear potential sweep for SAE 4140 steel electrode at 0.05 V s^{-1} in 0.05 M AOT and 0.10 M Py. Initial potential: 0.0 V. Starting in an anodic direction until reaching a value of 1.0 V (timeout of 90 s). Scans 1 (full line) and 5 (discontinuous line) are displayed. Small insert: scheme of the repetitive linear potential sweep applied.

micelles. The molecule has two bulky alkyl tails and a small negative charged SO_3^- headgroup.

In this article, results on the electropolymerization of a porous PPy films onto SAE 4140 steel in solutions containing AOT are presented. The effects of the electrosynthesis parameters on the PPy morphology are evaluated. The study is also focused on the incorporation of copper particles into the polymer matrix by a cementation process.

EXPERIMENTAL

Electrodes were prepared from SAE 4140 steel rod samples. The rods were embedded in a Teflon holder with an exposed area of 0.070 cm^2. Before each experiment, the exposed surfaces were polished to a 1000 grit finish using SiC, then degreased with acetone and washed with triply distilled water. Following this pretreatment, the electrode was immediately transferred to the electrochemical cell.
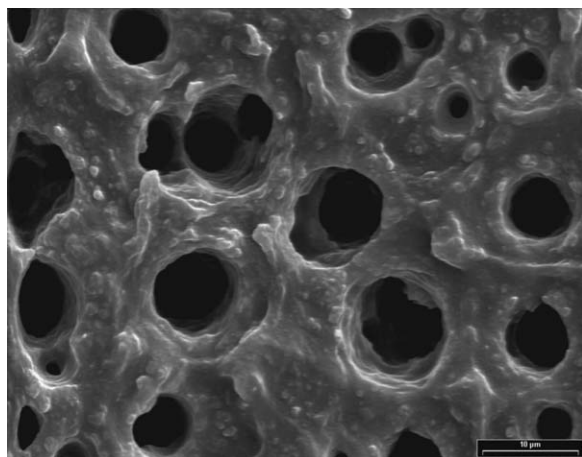

Figure 2. SEM micrograph of PPy$_{holes}$ film. The polymer was electrosynthesized in 0.05 M AOT and 0.10 M Py by applying the potential program described in Figure 1.

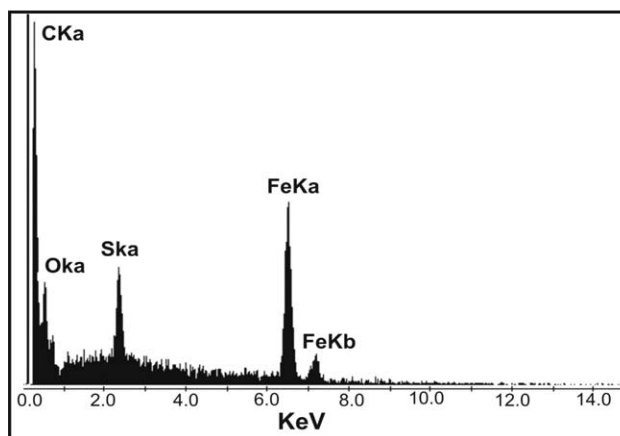**Figure 3.** EDX spectrum of PPy$_{holes}$ coating. The polymer was electrosynthesized in 0.05 M AOT and 0.10 M Py by applying the potential program described in Figure 1.

All the potentials were measured against a saturated Ag/AgCl and a platinum sheet was used as a counter electrode.

The cell was a 20-cm^3 Metrohm measuring cell. Electrochemical measurements were done using a potentiostat–galvanostat PAR
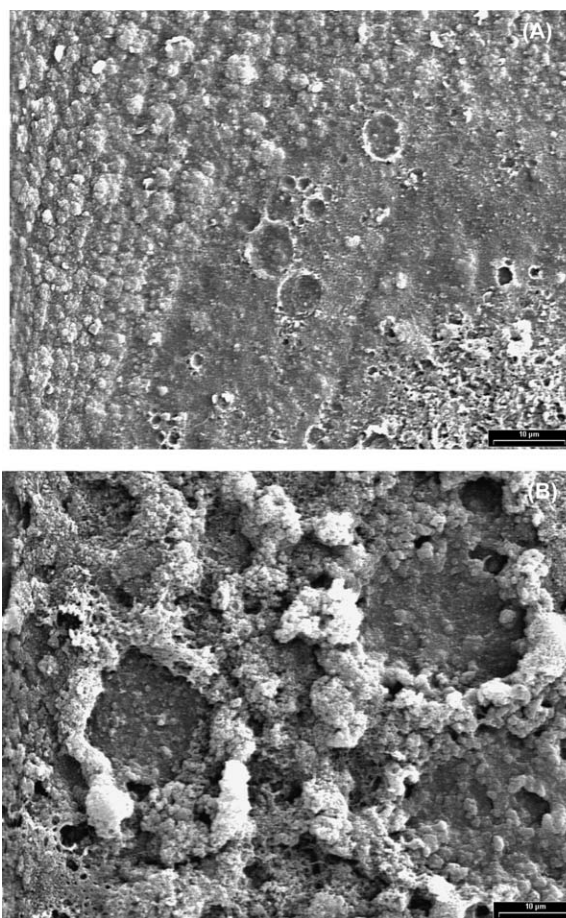

Figure 4. SEM micrographs of SAE/PPy. The polymer was electrosynthesized by a repetitive linear potential sweep at 0.05 V s^{-1} in 0.05 M AOT and 0.10 M Py. Initial potential: 0.0 V. Starting in an anodic direction until reaching a value of 1.0 V (timeout of 90 s), scan numbers: (A) 1 and (B) 2.
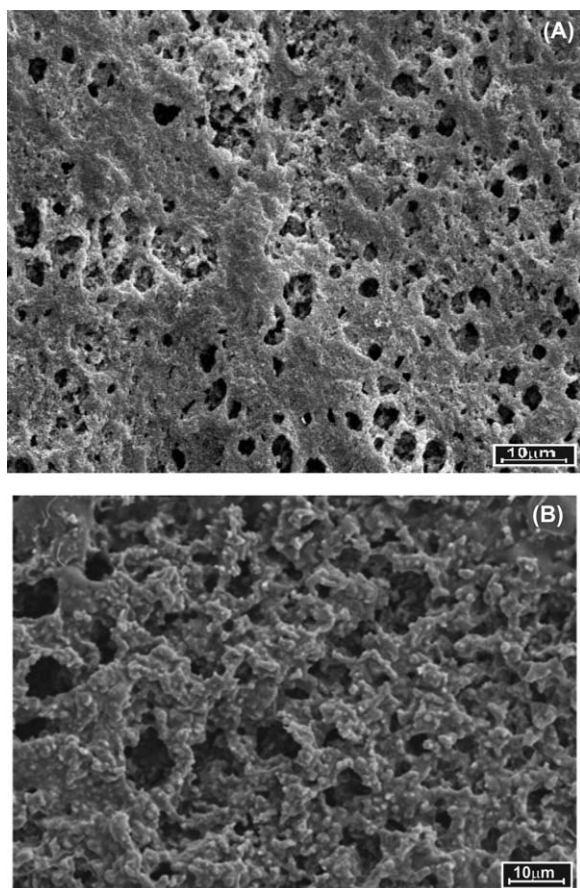
Figure 5. SEM micrographs of SAE/PPy. The polymer was electrosynthesized by applying the potential program described in Figure 1, in 0.05 *M* AOT and (A) 0.25 *M* Py and (B) 0.50 *M* Py.

Figure 6. SEM micrographs of SAE/PPy. (A) The polymer was electrosynthesized at 1.0 V for 450 s in 0.05 *M* AOT and 0.1 *M* Py (PPy$_{usual}$). (B) The polymer was electrosynthesized by a linear potential sweep at 0.05 V s^{-1} 0.05 *M* AOT and 0.1 *M* Py. Initial potential: 0.0 V. Starting in an anodic direction until reaching a value of 1.0 V (timeout of 450 s).

Model 273A and VoltaLab40 Potentiostat PGZ301. The frequency used for the impedance measurements was changed from 100 kHz to 10 mHz, and the signal amplitude was 10 mV. A dual stage ISI DS 130 SEM and an EDAX 9600 quantitative energy-dispersive X-ray analyzer were used to examine the PPy coatings. X-ray diffraction analysis was carried out using a Rigaku X-ray diffractometer (model Dmax III-C) with Cu Kα radiation and a graphite monochromator.

Electrical conductivity was measured by two-probe method using a homemade device and film adhesion was tested measuring the force necessary to peeloff the film using a Scotch® Magic^{TM} double coated Tape 810 (3 *M*) and a Mecmesin basic force gauge (BFG 50 N).

Measurements were performed in solutions containing pyrrole (Py) (0.01–1 *M*) and AOT (0.005–0.05 *M*) in a purified nitrogen gas saturated atmosphere at 20 °C, unless otherwise stated. The pH of the solution was adjusted by addition of NaOH. To avoid the slow hydrolysis of AOT all the measurements were done with freshly prepared samples. All chemicals were reagent grade and solutions were made in twice distilled water. Pyrrole was purchased from Aldrich and it was freshly distilled under reduced pressure before use.
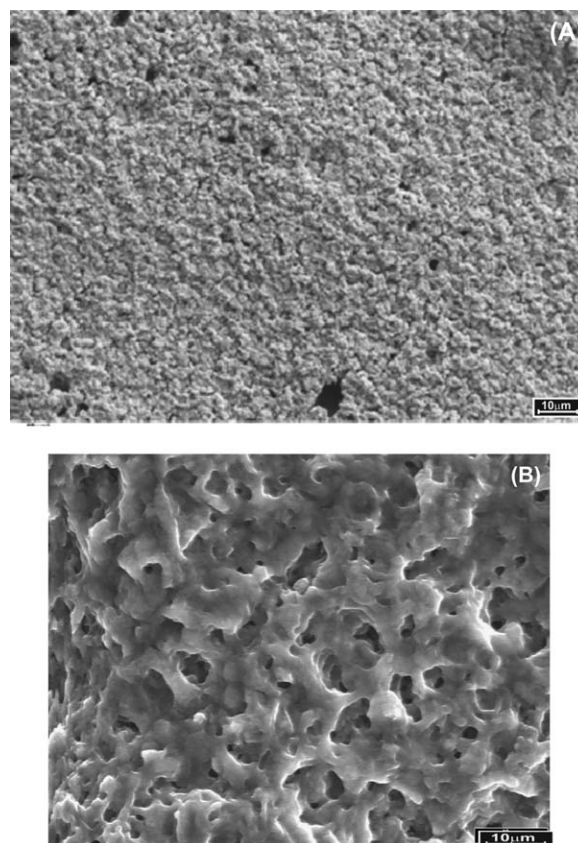
Each set of experiments was repeated two to four times to ensure reproducibility.

RESULTS AND DISCUSSION

Electrochemical Synthesis of PPy Film

A repetitive linear anodic potential scan with a potential holding at the more positive potential was applied for obtaining an
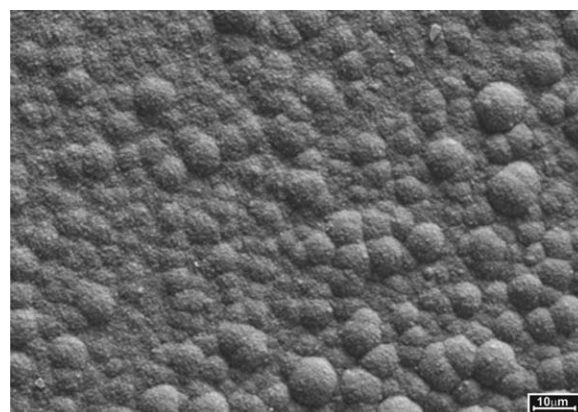

Figure 7. SEM micrograph of SAE/PPy. The polymer was electrosynthesized in 0.05 *M* SDBS and 0.10 *M* Py by applying the potential program described in Figure 1.
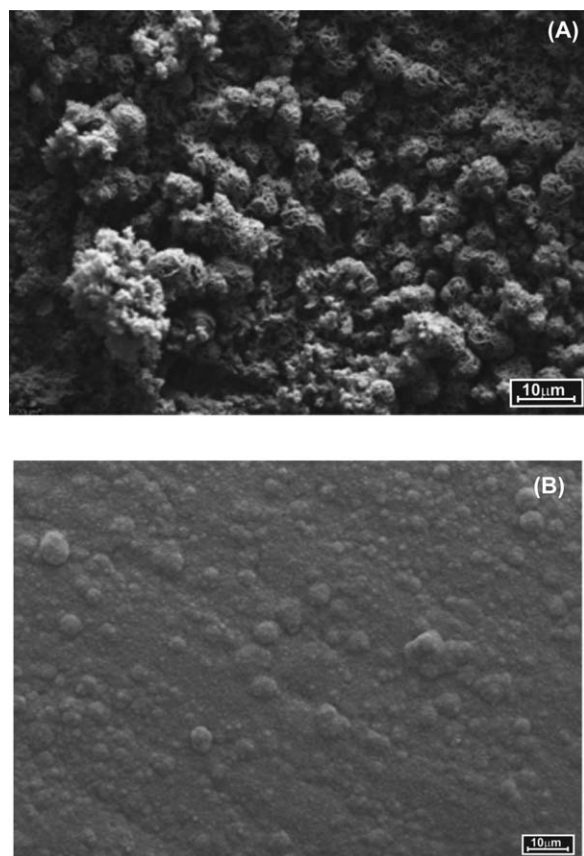
Figure 8. SEM micrographs of SAE/PPy. The polymer was electrosynthesized in 0.05 M AOT and 0.10 M Py by applying the potential program described in Figure 1, on: (A) iron and (B) vitreous carbon. Initial potential: 0.0 V.

adherent hole-containing coating (PPy$_{holes}$) on SAE 4140 in the presence of AOT. The resulting i versus E curves obtained after five scans starting in an anodic direction from 0.0 to 1.0 V

(timeout of 90 s) at 0.050 V s^{-1} in a solution containing 0.05 M AOT and 0.10 M Py are presented in Figure 1. When the potential is scanned from 0.0 V, the current increases at 0.7 V due to Py oxidation and subsequent polymerization. After scanning the sample surface is completely covered with a black coating. A SEM image shows the development of circular holes of diameter between 2 and 10 μm homogeneously distributed on the surface of the polymer (Figure 2). A gel material, can also distinguish on top of the coating. This material is a result of Fe dissolution and it was postulated that is a mixed NaAOT-Fe(AOT)$_3$ lamellar mesophase.[33] EDX analysis shows the presence of sulfur, indicating that AOT is present in both the polymer matrix and the gel material (Figure 3). Moreover, the Fe signal confirms the porous structure of the polymer.

To study the formation of the film with circular holes, the morphology of the polymer in the early stages of deposition was analyzed (Figure 4). Figure 4(A) shows the SEM image obtained after the first potential sweep was completed. The porous morphology obtained on SAE 4140 steel seems to initiate as worm-like fibrillar deposits that grow in a horizontal direction with respect to the substrate surface. The deposits grow during the second potential scan [Figure 4(B)]. These structures closely resemble those observed for PPy films electrosynthesized onto iron in 0.5 M Py with a low AOT concentration (0.005 M).[34]

When the Py concentration was 0.25 M randomly distributed irregular holes were observed [Figure 5(A)] while, for a concentration 0.50 M, the typical granular structure prevails [Figure 5(B)]. Small globules coexisting with some near-circular structures and a gelatinous product formed on top of the polymer are observed when the monomer concentration was lowered to 0.025 M.

The effect of the variation of AOT concentration in the electrosynthesis process was also tested. When the AOT concentration was 0.005 M, no polymer formation was observed while the gelatinous material covered the entire surface of the electrode. Only a partial covering of the surface by PPy was found when
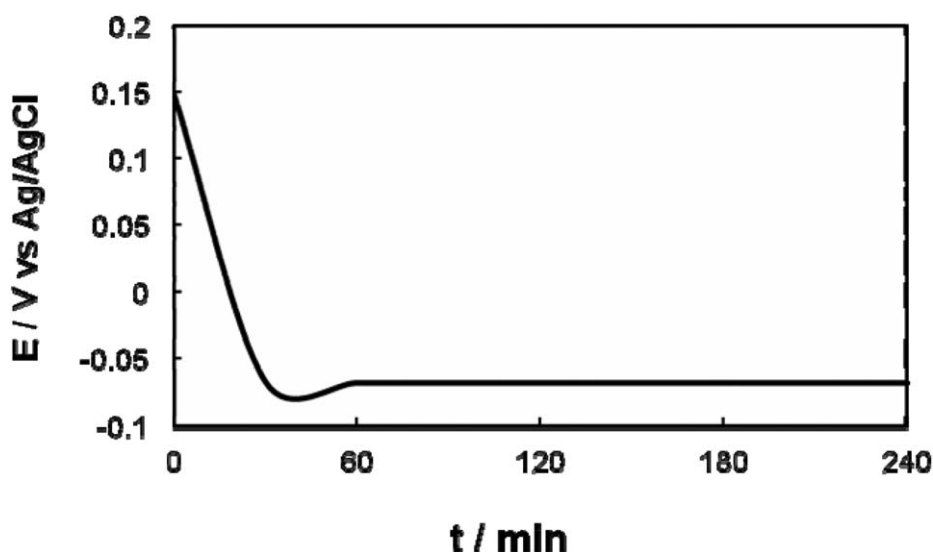

Figure 9. Time dependence of the OPC of a PPy$_{holes}$-coated steel electrode in 0.001 M Cu(NO$_3$)$_2$. The polymer was electrosynthesized in 0.05 M AOT and 0.10 M Py by applying the potential program described in Figure 1.
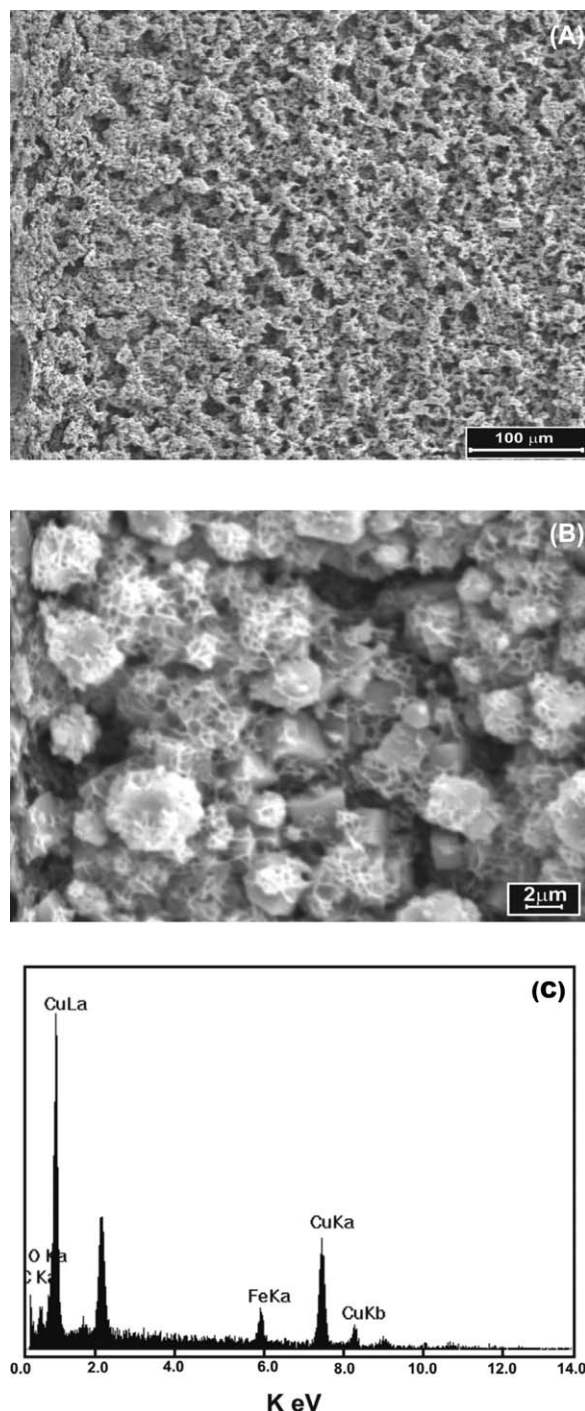
Figure 10. SEM micrographs of Cu-PPy$_{holes}$ film at different magnifications: (A) 1000× and (B) 6000×. The polymer was electrosynthesized in 0.05 M AOT and 0.10 M Py by applying the potential program described in Figure 1. The PPy film was modified by copper cementation in 0.0001 M Cu(NO$_3$)$_2$ during 240 min. (C) EDX spectrum of Cu-PPy$_{holes}$ coating.

the AOT concentration was 0.010 M. In this case, small grains of polymer and the gelatinous material were observed.

The potential program applied to the electrode also determines the morphology of the polymer. The formation of the characteristic grains of PPy (PPy$_{usual}$) is promoted when the electrodepo-

sition of PPy was performed by applying a potential of 1 V during 450 s [Figure 6(A)]. A single linear potential sweep with a potential holding at 1.0 V (timeout: 450 s) favored the development of a porous structure with few circular holes [Figure 6(B)].

To evaluate the effect of the surfactant in the polymer morphology, PPy films were also obtained in the presence of other surfactants: sodium dicyclohexyl sulfosuccinate (Aersol-a 196) and sodium dodecylbenzene sulfonate (SDBS). In both cases, PPy films show the usual grained structure (Figure 7).

One way to obtain a better comprehension of the phenomena involved in the formation of the PPy$_{holes}$ coating is to perform the electrodeposition onto another substrate by applying the same perturbation program. PPy electrodeposition onto iron leads to a morphology constituted by agglomerated platelets with dimensions in the order of 2 μm having a vertical alignment [Figure 8(A)]. This film was observed after an exhaustive washing with water to remove the gel material that covered the polymer completely. A compact and homogeneous morphology with the usual grained structure was obtained when the polymer is electrodeposited onto vitreous carbon [Figure 8(B)].

The obtained results indicate that the formation of a PPy$_{holes}$ film on SAE 4140 steel depends on the monomer and AOT concentrations, the chemical nature of the substrate, type of surfactant, and the perturbation program applied to the electrode. The formation of well-defined rings and microcontainers of PPy was explained by a self-assembled gas bubble template mechanism, where the bubbles correspond to hydrogen gas released from the counter electrode or oxygen gas produced on the working electrode.[35–39] Considering that the film with circular holes was not obtained employing iron or vitreous carbon as a substrate, the observed morphology does not seem to be the result of self-assembled gas bubble template growth mechanism. As was stated before, PPy structures presented in Figure 4 are very similar to those reported in a previous study, where the electrosynthesis of PPy was performed on iron in the presence of a lower AOT concentration.[34] It was proposed that worm-like fibrillar deposits grow until they bent forming near-circular structures. This kind of growth is favored at low
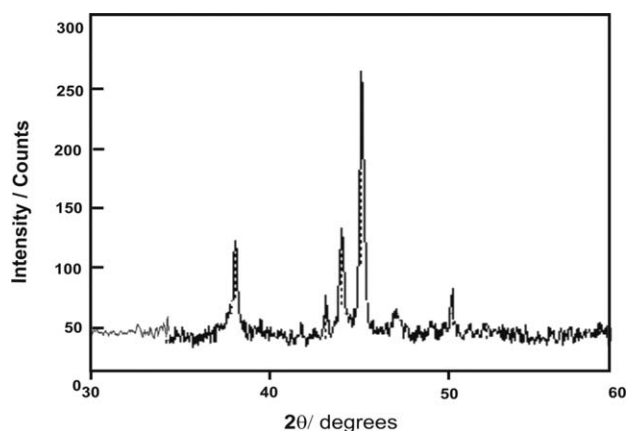

Figure 11. X-ray diffraction pattern of Cu-PPy$_{holes}$ film on SAE 4140 steel electrode. Diffraction lines due to the substrate (*).
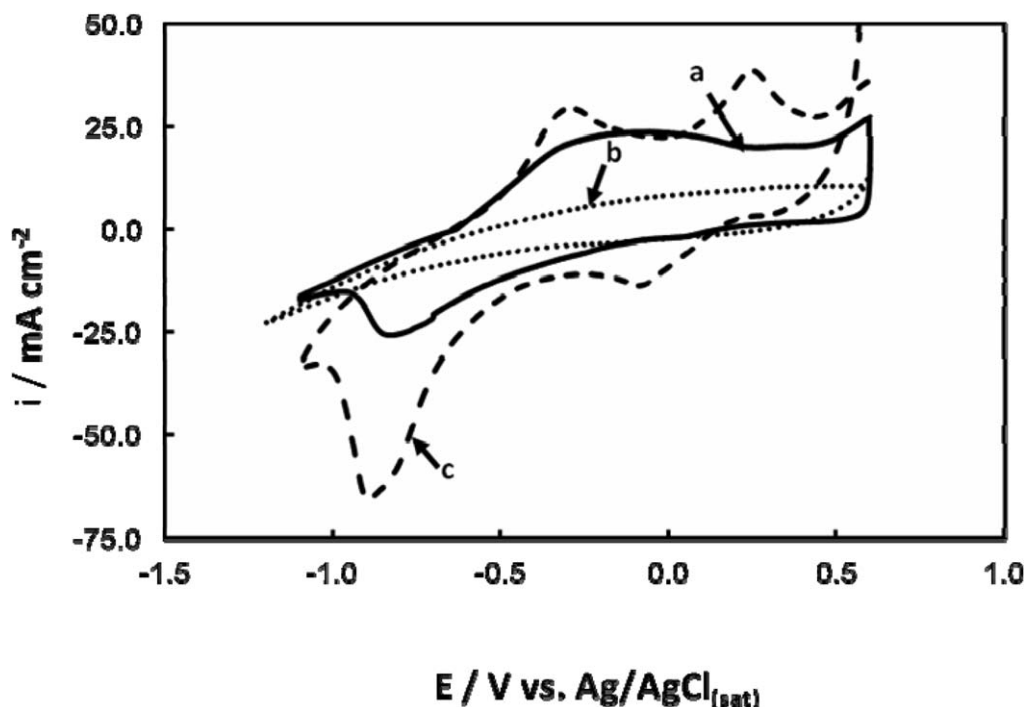
Figure 12. Cyclic voltammograms of PPy$_{holes}$-coated SAE 4140 steel electrode at 0.05 Vs^{-1} in 0.05 M AOT pH 7 for: (a) PPy$_{holes}$ coating, (b) PPy$_{usual}$ film, and (c) Cu-PPy$_{holes}$ film. The hole-containing polymer was electrosynthesized in 0.05 M AOT and 0.10 M Py by applying the potential program described in Figure 1. PPy$_{usual}$ coating was electropolymerized at 1 V during 450 s in 0.05 M AOT and 0.10 M Py.

electropolymerization rates. Likewise, AOT as a dopant promotes a more flexible polymer that allows the formation of the closed structures. Under the experimental conditions of the present work, the holes remain after the electropolymerization process was completed, that is they are not sealed by further polymer deposition.

PPy$_{holes}$ Film Modified by Copper Cementation

The incorporation of Cu particles into the PPy$_{holes}$ film was made in 0.0001 M Cu(NO$_3$)$_2$ pH 5, during 4 h under open cir-

Figure 13. The polarization behavior in 0.5 M NaCl at 0.001 V s^{-1} of: (a) PPy$_{holes}$ and (b) Cu-PPy$_{holes}$. The hole-containing polymer was electrosynthesized in 0.05 M AOT and 0.10 M Py by applying the potential program described in Figure 1. The modified PPy was obtained by cementation in 0.0001 M Cu(NO$_3$)$_2$ during 240 min.

cuit conditions. After 30 min of immersion the open circuit potential reaches—0.067 V which corresponds to the potential of the Cu^{2+}/Cu redox pair for 0.001 M Cu(NO$_3$)$_2$ (Figure 9). When the electrode is removed from the cell, the polymer is covered by a reddish brown top layer (Cu-PPy$_{holes}$). SEM analysis reveals that the film modified with Cu particles shows agglomerated structures of plate-like crystallites covering completely the polymer surface (Figure 10). A similar morphology was reported by other authors.[40]

Figure 10(C) presents the EDX spectrum confirming the presence of Cu in the PPy$_{holes}$ film. These results are consistent with the obtained X-ray diffraction of Cu-PPy$_{holes}$ films which reveal the formation of a crystalline structure where the diffraction peaks related to Cu are observed ($2\theta = 43.31$ and 50.43) (Figure 11).

Figure 12 shows the redox behavior of the unmodified PPy$_{holes}$ (curve a). The total charge involved is three times higher compared to the PPy with usual granular morphology (PPy$_{usual}$) obtained after polarization at 1.0 V during 450 s (Figure 12, curve b). The curve corresponding to Cu-PPy$_{holes}$ is also presented (Figure 12, curve c). The deposition of Cu particles leads to a significant increase in the total charge involved in the redox process. The more negative redox peaks are associated with Na$^+$ transport to conserve the electroneutrality of the film.[41] Additional anodic and cathodic current peaks are also distinguished. The cathodic peak at -0.17 V corresponds to the reduction of Cu^{2+} to Cu0 while the anodic one at about 0.20 V corresponds to Cu^0 oxidation.[42]

To establish the chemical state of copper in the coating, anodic and cathodic stripping sweeps starting at 0.1 V in 0.05 M AOT
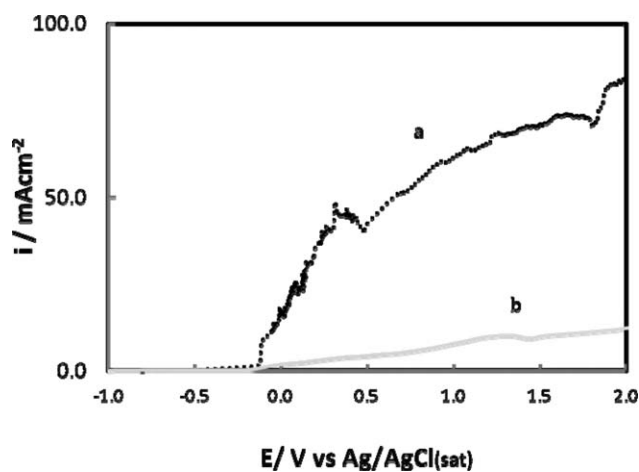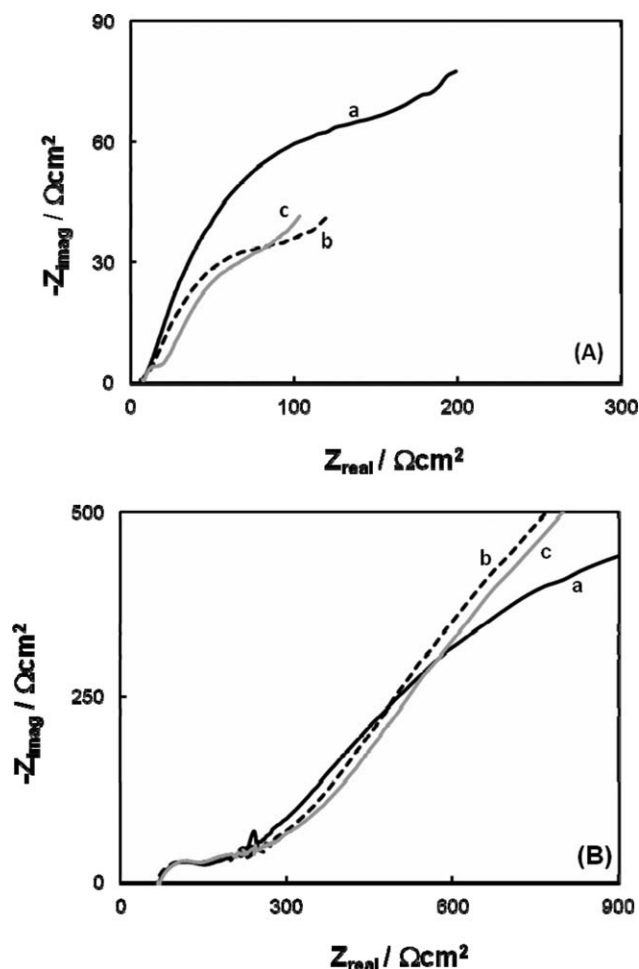
Figure 14. Nyquist plots of the impedance spectra for the samples at the open circuit potential in 0.5 M NaCl after different immersion times: (A) PPy$_{holes}$, (a) 5 min ($E_{OCP} = -0.29$ V), (b) 60 min ($E_{OCP} = -0.49$ V), and (c) 90 min ($E_{OCP} = -0.52$ V) and (B) Cu-PPy$_{holes}$, (a) 5 min ($E_{OCP} = -0.18$ V), (b) 90 min ($E_{OCP} = -0.25$ V), and (c) 360 min ($E_{OCP} = -0.49$ V).

at 0.001 V s^{-1} (not shown). The obtained results allow to conclude that metallic and ionic copper species are present in the coating. The formation of a complex compound between Cu^{2+} and AOT is reported in the literature.[43] In this way, Cu^{2+} ions can be concentrated in the film. With respect to the deposition of metallic Cu, it can be proposed that the oxidation reaction that occurs simultaneously with the Cu^{2+} ions reduction is the oxidation of non-oxidized segments within the polymer. This option seems to be unlikely since deposition of Cu under open potential circuit conditions occurred even when the polymer was in the overoxidized state. Another possibility is iron oxidation. This option is feasible considering the structure of hole-containing PPy film. It was not possible to deposit Cu on the PPy formed with granular morphology (PPy$_{usual}$). In this case, the more closed and compact structure of the polymer hinders the transport of iron ions.

Electrical conductivity values for PPy$_{holes}$ and Cu- PPy$_{holes}$ films are 4.29×10^{-3} S cm^{-1} and 9.42×10^{-3} S cm^{-1}, respectively. These results show that the PPy$_{holes}$ film modified with Cu have

better electrical conductivity than the unmodified polymer. This enhanced conductivity of the samples is due to the incorporation of metal particles into the polymer matrix. The combination of amorphous and crystalline structure in the composite material may also be the reason for improved conductivity.[44] The increased redox charge registered for the modified film is probably related to its better conductivity (Figure 12, curve c).

To compare the adhesion force property of the unmodified and modified PPy$_{holes}$ coatings the necessary force to peel-off the films was measured. The obtained values were 23.50 N for PPy$_{holes}$ and 34.45 N for Cu-PPy$_{holes}$ film. Thus, the presence of Cu improves the adhesion of the hole-containing PPy films. Both coatings can be removed only by mechanical polishing.

The corrosion behavior of the substrates was investigated in 0.5 M NaCl solution by a linear polarization method and electrochemical impedance spectroscopy (EIS). Anodic polarization curves of the SAE 4140 electrode covered by unmodified and modified PPy with Cu obtained at 0.001 V s^{-1} are presented in Figure 13. The curve for the unmodified polymer shows a current increase at -0.12 V related to the pitting corrosion (Figure 13, curve a). In the case of the Cu-PPy$_{holes}$ film a significative increase in the anodic current can be observe at more anodic potential values (Figure 13, curve b).

The impedance spectra for the different systems in 0.5 M NaCl solutions are present in Figure 14. It is interesting to note that the total impedance increased with the immersion time in all cases except for PPy$_{holes}$ coating [Figure 14(A)]. Diffusional phenomena are visible only in the spectra of the Cu-PPy$_{holes}$ film. The linear part in the low-frequency region of Bode plot is associated with the characteristics of a corrosion reaction inhibited by mass transfer limitations.[45] This response means that the film behaves as a blocked electrode.

The obtained results indicate that the presence of Cu improves the anticorrosive performance of hole-containing PPy film. The better anticorrosion efficiency can be explained considering that pores in the polymer are quite effectively sealed.[46] Likewise, the
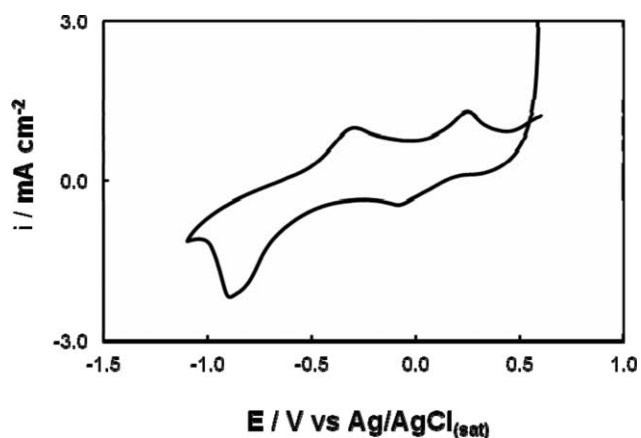

Figure 15. Cyclic voltammograms of Cu-PPy$_{holes}$ at 0.05 V s^{-1} in 0.05 M AOT pH 7. The hole-containing polymer was electrosynthesized in 0.05 M AOT and 0.10 M Py by applying the potential program described in Figure 1 and after that it was immersed in 1×10^{-7} M Cu(NO$_3$)$_2$ solution during 10 h.
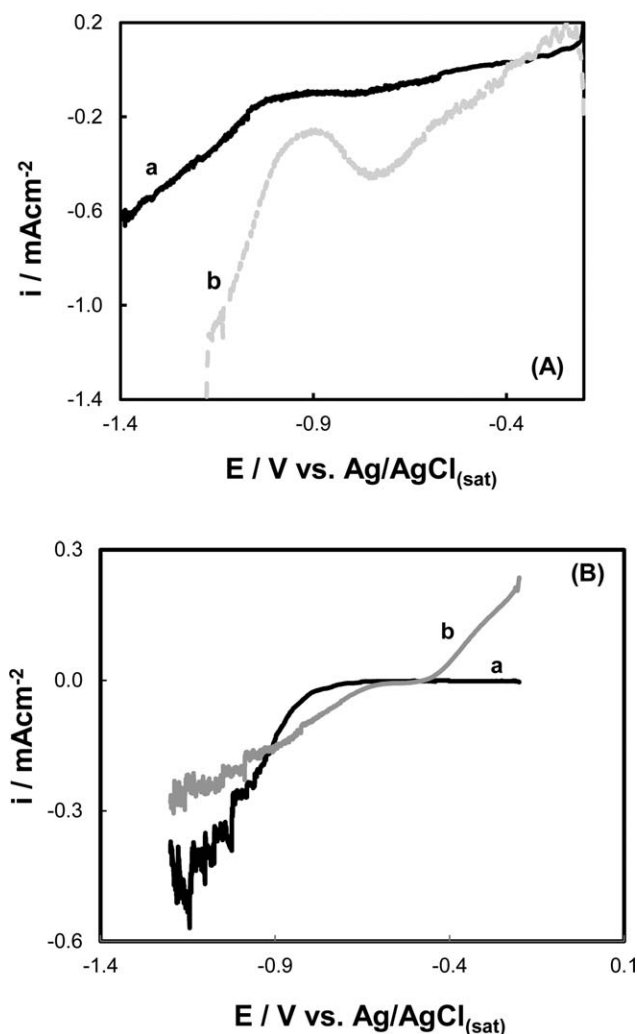
Figure 16. Cathodic polarization curves in 0.1 M H$_2$SO$_4$ solution at 0.001 V s^{-1} for: (A) (a) PPy$_{holes}$ and (b) Cu-PPy$_{holes}$. (B) Uncoated Cu (curve a) and SAE 4140 steel (curve b).

anticorrosive properties provided by conducting polymers are related to the galvanic interaction between the metallic substrate and the coating which ensures the presence of the passive film.[47,48] Then, the conductive state of the polymer is a fundamental requirement and in this sense, the conductivity of the coating increases in the presence of Cu.

Preliminary Evaluation of the Potential Applications of the Coatings Studied

Copper Removal and Recovery by Cementation Process. The cementation method is an attractive way to recover copper of wastewaters. The PPy$_{holes}$ coating was immersed during 12 h in a solution containing 1×10^{-7} M Cu^{2+} ions. As shown in Figure 15, the current peaks associated to the presence of Cu species can be detected. The charges related to the oxidation and reduction process are 11.4 and 4.4 mC/cm^2, respectively. The results point toward a simple and low cost method for Cu recovery.

Electrocatalytic Activity of PPy Films. The hydrogen evolution reaction (HER) activity of resulting PPy$_{holes}$ unmodified and

modified with Cu was evaluated by a potentiodynamic sweep in 0.1 M H$_2$SO$_4$ solution at 0.001 V s^{-1} [Figure 16(A)]. The curves have a similar shape but a significant increase in the registered current was observed for the sample containing Cu. When the electrode is removed from the cell the acid solution did not present the typical yellow coloration indicative of iron dissolution. The Cu-PPy$_{holes}$ is a much better catalyst than bare steel and copper electrodes [Figure 16(B)].

CONCLUSIONS

A simple method for the electrodeposition of hole-containing PPy films onto SAE 4140 steel was employed. The formation of this type of polymer structure depends on the nature of the substrate, type of surfactant and the employed electrochemical technique. The hole-containing coating allows the incorporation of copper particles by cementation, which increases the surface area. The obtained results point towards a simple, low cost, and highly sensitive method for Cu recovery. Moreover, the hole-containing coating is a promising matrix for the incorporation of several other metals.

The copper deposits and its corrosion products enhance the corrosion protection of the substrate hindering the transport of aggressive ions. The electrical conductivity of the PPy$_{holes}$ increases by the copper cementation favoring the galvanic interaction with the substrate.

Cu-PPy$_{holes}$ coating shows a better catalytic performance for the proton reduction in comparison with the unmodified PPy$_{holes}$ film.

ACKNOWLEDGMENTS

REFERENCES

1. Yang, C.; Liu, P.; Guo, J.; Wang, Y. *Synth. Met.* **2010**, *160*, 592.

2. Majid, K.; Tabassum, R.; Shah, A. F.; Ahmad, S.; Singla, M. L. *J. Mater. Sci. Mater. Electron.* **2009**, *20*, 958.

3. Basavaraja, C.; Veeranagouda, Y.; Lee, K.; Vishnuvardhan, T. K.; Pierson, R.; Huh, D. S. *J. Polym. Res.* **2010**, *17*, 233.

4. Wei, S.; Mavinakuli, P.; Wang, Q.; Chen, D.; Asapu, R.; Mao, Y.; Haldolaarachchige, N.; Young, D. P.; Guo, Z. *J. Electrochem. Soc.* **2011**, *158*, K205.

5. Ding, K.; Jia, H.; Wei, S.; Guo, Z. *Ind. Eng. Chem. Res.* **2011**, *50*, 7077.

6. Saremi, M.; Salehisaki, M. *Electroanalysis* **2014**, *26*, 1606.

7. Stoian, A. B.; Buica, G. O.; Demetrescu, I. *J. Appl. Polym. Sci.* **2015**, *132*, DOI: 10.1002/app.41375.

8. Khaniche, B.; Benamrani, H.; Zouaoui, A.; Zegadi, A. *Mater. Sci. Semicond. Process.* **2014**, *27*, 689.

9. Warren, R.; Sammoura, F.; Teh, S. K.; Kozinda, A.; Zang, X.; Lin, L. *Sens. Actuators A* **2015**, *231*, 65.

10. Hatchett, D. W.; Josowicz, M. *Chem. Rev.* **2008**, *108*, 746.

11. Bangar, M. A.; Chen, W.; Myung, N. V.; Mulchandani, A. *Thin Solid Films* **2010**, *519*, 964.

12. Grari, O.; Et Taouil, A.; Dhouibi, L.; Buron, C. C.; Lallemand, F. *Prog. Org. Coat.* **2015**, *88*, 48.

13. Bazzaoui, M.; Martins, J. I.; Bazzaoui, E. A.; Albourine, A.; Martins, L. *Mater. Corros* **2014**, *65*, 67.

14. Ivanov, S.; Tsakova, V. *Electrochim. Acta* **2005**, *50*, 5616.

15. González, M. B.; Brugnoni, L. I.; Vela, M. E.; Saidman, S. B. *Electrochim. Acta* **2013**, *102*, 66.

16. Aitout, R.; Makhloufi, L.; Saidani, B. *Thin Solid Films* **2006**, *515*, 1992.

17. Ramesan, M. T. *J. Appl. Polym. Sci.* **2013**, *128*, 1540.

18. Ulubay, S.; Dursun, Z. *Talanta* **2010**, *80*, 1461.

19. Rapecki, T.; Donten, M.; Stojek, Z. *Electrochem. Commun.* **2010**, *12*, 624.

20. Mathiyarasu, J.; Senthilkumar, S.; Phani, K. L. N.; Yegnaraman, V. *Mater. Lett.* **2008**, *62*, 571.

21. Tsakova, V.; Borissov, D. *Electrochem. Commun.* **2000**, *2*, 511.

22. Pournaghi-Azar, M. H.; Ojani, R. *J. Solid State Electrochem.* **1999**, *3*, 392.

23. Tamm, J.; Alumaa, A.; Hallik, A.; Johanson, U.; Tamm, T. *Russ. J. Electrochem.* **2002**,

24. Yuan, Y. J.; Adeloju, S. B.; Wallace, G. G. *Eur. Polym. J.* **1999**, *35*, 1761.

25. Nguyen-Cong, H.; Abbassi, K. E. I.; Gautier, J. L.; Chartier, P. *Electrochim. Acta* **2005**, *50*, 1369.

26. Singh, R. N.; Lal, B.; Malviya, M. *Electrochim. Acta* **2004**, *49*, 4605.

27. Gautier, J. L.; Marco, J. F.; Gracia, M.; Gancedo, J. R.; de la Garza Guadarrama, V.; Nguyen-Cong, H.; Chartier, P. *Electrochim. Acta* **2002**, *48*, 119.

28. Nguyen-Cong, H.; de la Garza Guadarrama, V.; Gautier, J. L.; Chartier, P. *Electrochim. Acta* **2003**, *48*, 2389.

29. Makhloufi, L.; Hammache, H.; Saidani, B. *Electrochem. Commun.* **2000**, *2*, 552.

30. Lehr, I. L.; Saidman, S. B. *Mater. Chem. Phys.* **2006**, *100*, 262.

31. Lehr, I. L.; Saidman, S. B. *Corros. Sci.* **2007**, *49*, 2210.

32. Flamini, D. O.; Saidman, S. B. *Electrochim. Acta* **2010**, *55*, 3727.

33. Lehr, I. L.; Saidman, S. B. *Prog. Org. Coat.* **2013**, *76*, 1586.

34. Lehr, I. L.; Saidman, S. B.; Schulz, P. C. *J. Colloid Interf. Sci.* **2007**, *306*, 323.

35. Lehr, I. L.; Saidman, S. B. *Synth. Met.* **2009**, *159*, 1522.

36. Qu, L.; Shi, G.; Chen, F.; Zhang, J. *Macromolecules* **2003**, *36*, 1063.

37. Chen, G.; Tallman, D. E.; Bierwagen, G. P. *J. Solid State Electrochem.* **2004**, *8*, 505.

38. Lemon, P.; Haigh, J. *Mater. Res. Bull.* **1999**, *34*, 665.

39. Qu, L.; Shi, G.; Yuan, J.; Han, G.; Chen, F. *J. Electroanal. Chem.* **2004**, *561*, 149.

40. Orináková, R.; Filkusová, M. *Synth. Met.* **2010**, *160*, 927.

41. Ozkazanc, E. *Synth. Met.* **2012**, *162*, 1016.

42. Saidman, S. B. *Electrochim. Acta* **2003**, *48*, 1719.

43. Zanganeh, A.; Amini, M. *Sens. Actuators B* **2008**, *135*, 358.

44. Eastoe, J.; Fragneto, G.; Robinson, B. H.; Towey, T. F.; Heenan, R. K.; Leng, F. J. *J. Chem. Soc. Faraday Trans.* **1992**, *88*, 461.

45. Straumal, B. B.; Protasova, S. G.; Mazilkin, A. A.; Baretzky, B.; Myatiev, A. A.; Straumal, P. B.; Tietze, T.; Schütz, G.; Goering, E. *Mater. Lett.* **2012**, *71*, 21.

46. Lehr, I. L.; Saidman, S. B. *React. Funct. Polym.* **2008**, *68*, 1152.

47. Tüken, T. *Prog. Org. Coat.* **2006**, *55*, 60.

48. Biallozor, S.; Kupniewska, A. *Synth. Met.* **2005**, *155*, 443.

49. Hermas, A. A. *Corros. Sci.* **2008**, *50*, 2498.